Biochem. J. (2013) **449**, 167–173 (Printed in Great Britain) doi:10.1042/BJ20121271

Cytosolic [Ca^{2+}] regulation of InsP_3-evoked puffs

Michiko YAMASAKI-MANN*[1], Angelo DEMURO* and Ian PARKER*†

*Department of Neurobiology and Behavior, University of California, Irvine, CA 92697, U.S.A., and †Department of Physiology and Biophysics, University of California, Irvine, CA 92697, U.S.A.

InsP_3-mediated puffs are fundamental building blocks of cellular Ca^{2+} signalling, and arise through the concerted opening of clustered InsP_3Rs (InsP_3 receptors) co-ordinated via Ca^{2+}-induced Ca^{2+} release. Although the Ca^{2+} dependency of InsP_3Rs has been extensively studied at the single channel level, little is known as to how changes in basal cytosolic [Ca^{2+}] would alter the dynamics of InsP_3-evoked Ca^{2+} signals in intact cells. To explore this question, we expressed Ca^{2+}-permeable channels (nicotinic acetylcholine receptors) in the plasma membrane of voltage-clamped *Xenopus* oocytes to regulate cytosolic [Ca^{2+}] by changing the electrochemical gradient for extracellular Ca^{2+} entry, and imaged Ca^{2+} liberation evoked by photolysis of caged InsP_3. Elevation of basal cytosolic [Ca^{2+}] strongly increased the amplitude and shortened the latency of global Ca^{2+} waves. In oocytes loaded with EGTA to localize Ca^{2+} signals, the number of sites at which puffs were observed and the frequency and latency of puffs were strongly dependent on cytosolic [Ca^{2+}], whereas puff amplitudes were only weakly affected. The results of the present study indicate that basal cytosolic [Ca^{2+}] strongly affects the triggering of puffs, but has less of an effect on puffs once they have been initiated.

Key words: Ca^{2+} puffs, cytosolic Ca^{2+}, InsP_3, InsP_3 receptor (InsP_3R).

INTRODUCTION

The InsP_3R (InsP_3 receptor) is a Ca^{2+}-permeable channel expressed in the ER (endoplasmic reticulum) which is gated by the binding of the second messenger InsP_3 and by cytosolic Ca^{2+} itself [1–7]. Ca^{2+} liberation occurs at discrete functional release sites, formed by clusters of InsP_3R on the ER membrane. These participate in generating a hierarchy of cellular Ca^{2+} signals involving opening of single InsP_3R channels [8,9], concerted release from several channels within a cluster [10] and global Ca^{2+} waves that propagate from cluster to cluster [11,12]. The positive-feedback mechanism of CICR (Ca^{2+}-induced Ca^{2+} release), by which Ca^{2+} released from one InsP_3R channel promotes opening of neighbouring channels, underlies these processes, and factors including cytosolic Ca^{2+} buffering, [InsP_3] and basal cytosolic [Ca^{2+}] determine the transition between local and global signalling patterns.

The role of cytosolic Ca^{2+} in modulating InsP_3R channel gating has been extensively studied by single-channel recordings from InsP_3R in excised nuclei and after reconstitution in lipid bilayers, revealing the well-known 'bell-shaped' curve of Ca^{2+} facilitation and inhibition [1,2,13,14]. However, less is known of how cytosolic Ca^{2+} modulates local InsP_3-mediated signals in the intact cell, although imaging studies in *Xenopus* oocytes demonstrate a profound potentiation of global Ca^{2+} waves [13,15–17].

In the present study, we expressed Ca^{2+}-permeable nAChRs (nicotinic acetylcholine receptor/channels) in the plasma membrane of *Xenopus* oocytes so as to experimentally regulate the basal cytosolic [Ca^{2+}] concentration [18], and examined how elevations in cytosolic [Ca^{2+}] affected the dynamics of local and global Ca^{2+} signals evoked by photoreleased InsP_3. We show that an increased probability of triggering local Ca^{2+} release at puff sites underlies the strong augmentation of global InsP_3-mediated Ca^{2+} waves, whereas puff amplitudes and durations were unaffected.

EXPERIMENTAL

Oocyte preparation and expression of nAChRs

Xenopus laevis were purchased from Nasco International and the oocytes were surgically removed [19] following protocols approved by the UC Irvine Institutional Animal Care and Use committee. Stage V–VI oocytes were isolated and treated with collagenase (1 mg/ml collagenase type A1 for 30 min) to remove the follicular cell layers. At 1 day after isolation the oocytes were injected with a cRNA mixture for nAChR expression (α, β, γ and δ subunits at a ratio of 2:1:1:1; 50 nl at a final concentration of 0.1–1 mg/ml) and were then maintained in modified Barth's solution [88 mM NaCl, 1 mM KCl, 2.4 mM $NaHCO_3$, 0.82 mM $MgSO_4$, 0.33 mM $Ca(NO_3)_2$, 0.41 mM $CaCl_2$, 5 mM Hepes and 1 mg/ml gentamicin (pH 7.4)] for 1–3 days at 16 °C before use. Expression of nAChRs was evaluated using a voltage clamp to measure the currents evoked by 500 nM ACh: oocytes showing currents >1 μA at -80 mV were selected for the experiments.

Microinjection of oocytes

Intracellular microinjections were performed using a Drummond microinjector. Approximately 1 h before the Ca^{2+} imaging experiments, oocytes in Ca^{2+}-free Barth's solution were injected with Fluo-4 dextran (high affinity; $K_d = 800$ nM) to a final concentration of 40 μM, assuming equal distribution throughout

Abbreviations used: CCD, charge-coupled device; CICR, Ca^{2+}-induced Ca^{2+} release; ER, endoplasmic reticulum; FDHM, full duration at half-maximal amplitude; InsP_3R, InsP_3 receptor; nAChR, nicotinic acetylcholine receptor/channel; SERCA, sarcoplasmic/ER Ca^{2+}-ATPase.

[1] To whom correspondence should be addressed at the present address: Department of Physiology, Anatomy and Genetics, University of Oxford, Le Gros Clark Building, South Parks Road, Oxford, U.K. (email michiko.yamasaki-mann@dpag.ox.ac.uk).

a cytosolic volume of 1 μl and with caged Ins(1,4,5)P_3,P$^{4(5)}$-[1-(2-nitrophenyl)ethyl]ester (final concentration 8 μM). EGTA (final concentration 300 μM) was further injected for puff studies.

Ca^{2+} imaging and flash photolysis

Oocytes were voltage-clamped using a conventional two-microelectrode technique. The membrane potential was held at 0 mV during superfusion with a non-desensitizing concentration of ACh (100–500 nM) in Ringer's solution and was briefly stepped to -120 mV to strongly increase the electrical driving force for Ca^{2+} influx [20]. Global Ca^{2+} signals were imaged at room temperature (18–20 °C) by a custom-build confocal line scanner [21] interfaced to an Olympus inverted microscope IX 70, and fluorescence excitation was provided by the 488 nm line of an argon ion laser, with the laser spot focused by a $\times 40$ oil-immersion objective [NA (numerical aperture) = 1.35] and scanned along at a rate of 10 ms/50 μm line. To image puffs, we used wide-field fluorescence microscopy using an Olympus IX 71 inverted microscope equipped with a $\times 40$ oil-immersion objective, a 488 nm argon ion laser for fluorescence excitation and an electron-multiplied CCD (charge-coupled device) camera (Cascade 128+; Roper Scientific) for imaging fluorescence emission (510–600 nm) at a frame rate of 500 s^{-1}. Fluorescence was imaged from a 40 μm $\times$ 40 μm (128 $\times$ 128 pixel) region within the animal hemisphere of the oocyte. Fluorescence measurements made by line-scan and camera imaging are expressed as a ratio ($\Delta F/F_0$) of the mean change in fluorescence (ΔF) at a pixel relative to the resting fluorescence at that pixel before stimulation (F_0). The mean values of F_o were obtained by averaging over several scans/frames before stimulation. To calibrate the changes in $\Delta F/F_0$ values in terms of nanomolar increases of free [Ca^{2+}] we determined maximal (F_{max}) and minimal (F_{min}) fluorescence values by injecting fluo-4 dextran-loaded oocytes ($n = 5$) with 30 nl of 100 mM $CaCl_2$ or 100 mM EGTA from a micropipette located close to the imaging site. After correcting for oocyte autofluorescence, the mean values were $F_{max} = 8.52 \pm 1.16$ and $F_{min} = 0.857 \pm 0.024$ relative to the resting fluorescence F_0 before injection. We assumed a K_d value for fluo-4 dextran of 2400 nM, based on measurements of $\sim$800 nM in free solution [22] and a roughly 3-fold reduction in affinity in the cytoplasmic environment [22]. A fluorescence increase of $\Delta F/F_o = 1$ above baseline would then correspond to an increase of $[Ca^{2+}]_{cyt}$ of about 360 nM. Photolysis of caged InsP_3 was evoked by flashes of UV light (350–400 nm) from a mercury arc lamp, delivered through the microscope objective and adjusted to uniformly irradiate a circular region slightly larger than the imaging frame or scan line. Flash durations were set using a Uniblitz shutter and digital controller.

Reagents

Fluo-4 dextran (high affinity; K_d $\sim$800 nM), and caged InsP_3 were purchased from Invitrogen. All other reagents were from Sigma–Aldrich.

Data analysis

Custom routines written in the IDL programming environment (Research Systems) were used for linescan image processing and measurements. MetaMorph (Molecular Devices) was used to process and measure data obtained from wide-field camera-based imaging. Further analysis and graphing was accomplished using Microcal Origin version 6.0 (OriginLab). Results are means $\pm$ S.E.M. and significance was assessed by Student's t test.

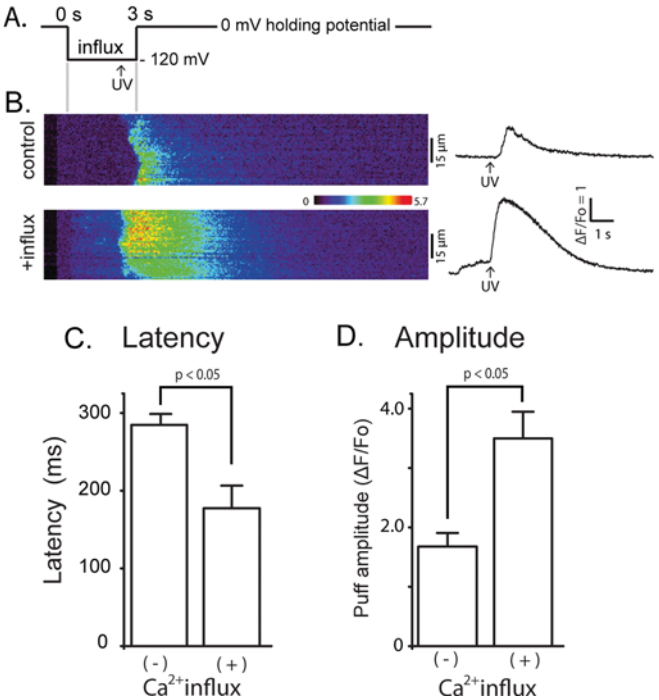

Figure 1 Elevated basal cytosolic [Ca^{2+}] enhances InsP_3-induced Ca^{2+} waves

(**A**) Schematic diagram of the experimental protocol. (**B**) Representative confocal linescan images illustrating fluo-4 dextran fluorescence signals evoked by photoreleased InsP_3 under control conditions without elevation of cytosolic [Ca^{2+}] (upper panel) and with cytosolic [Ca^{2+}] elevation (lower panel). Increasing fluorescence ($\Delta F/F_0$ and Ca^{2+} level) is depicted on a pseudocolour scale as indicated by the colour bar. The traces on the right-hand side show corresponding fluorescence profiles averaged across 15 μm widths of the linescans (indicated by bars). (**C**) Mean values of latency between the photolysis flash and initial rise in fluorescence derived from traces like those in (**B**). Latency without Ca^{2+} influx = 284 $\pm$ 14 ms and during Ca^{2+} influx = 177 $\pm$ 30 ms; $P < 0.05$. (**D**) Mean peak amplitudes of Ca^{2+} waves derived from traces like those in (**B**). $\Delta F/F_0$ without Ca^{2+} influx = 1.68 $\pm$ 0.23 and during Ca^{2+} influx = 3.50 $\pm$ 0.45; $P < 0.05$, $n = 6$ and 4 oocytes respectively. In (**C**) and (**D**) the results are means $\pm$ S.E.M.

RESULTS

Elevated basal cytosolic [Ca^{2+}] enhances InsP_3-evoked Ca^{2+} waves

In order to evoke cytosolic [Ca^{2+}] elevations, Ca^{2+} influx was induced through nAChRs expressed in the oocyte plasma membrane. Oocytes were continuously superfused with Ringer's solution containing 1.8 mM Ca^{2+}, together with a low non-desensitizing concentration (100–500 nM) of acetylcholine, and were voltage-clamped to control the electrochemical gradient for Ca^{2+} entry. The membrane potential was held at 0 mV to minimize Ca^{2+} influx, and was then stepped to more negative values to promote Ca^{2+} influx beginning 2.5 s before the delivery of a UV flash to photorelease InsP_3 from a caged precursor loaded into the oocyte (Figure 1A). The resulting changes in fluo-4 fluorescence were imaged to compare InsP_3-evoked Ca^{2+} responses evoked by identical UV flashes during cytosolic [Ca^{2+}] elevation with control records when the voltage pulse was not applied.

We first examined global Ca^{2+} signals evoked in oocytes that were not loaded with EGTA. The panels on the left-hand side of Figure 1(B) show representative linescan images of fluorescence

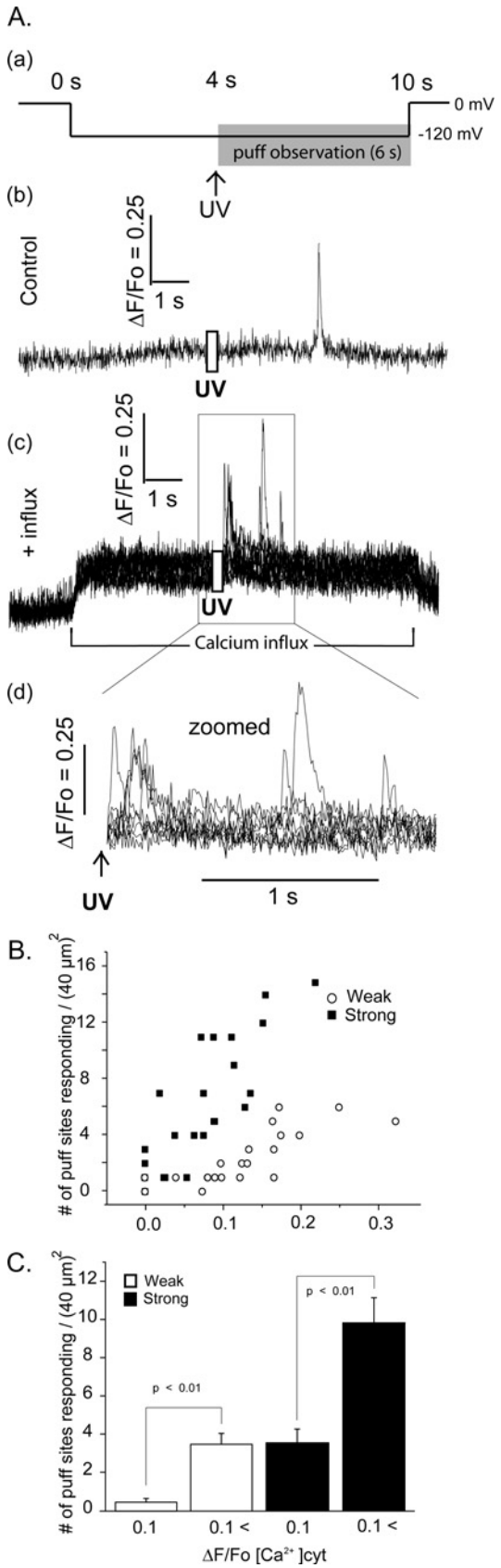

Figure 2 Cytosolic $[Ca^{2+}]$-dependent potentiation of InsP_3-evoked Ca^{2+} puffs

changes evoked by photoreleased InsP_3 without (upper panel) and with (lower panel) Ca^{2+} influx; the corresponding fluorescence profiles are presented on the right-hand side. We compared the latencies and peak amplitude of InsP_3-evoked Ca^{2+} signals under resting cytosolic $[Ca^{2+}]$, and during Ca^{2+} influx that increased the basal fluorescence signal by a mean of 0.60 ± 0.06 $\Delta F/F_o$ (six oocytes from three different frogs). Latencies (time from the UV flash to the initial rise in fluorescence) were significantly shorter during cytosolic $[Ca^{2+}]$ elevation (Figure 1C; control latency $= 284 \pm 14$ ms and during Ca^{2+} influx latency $= 177 \pm 30$ ms; $P < 0.05$). The mean peak amplitude of Ca^{2+} waves was profoundly augmented by cytosolic Ca^{2+} elevation (Figure 1D; control $\Delta F/F_o = 1.68 \pm 0.23$ and during Ca^{2+} influx $\Delta F/F_0 = 3.50 \pm 0.45$; $P < 0.05$, $n = 6$). These results are consistent with previous observations showing facilitation of InsP_3-evoked Ca^{2+} signals by cytosolic $[Ca^{2+}]$ [1–7].

Elevated basal cytosolic $[Ca^{2+}]$ promotes InsP_3-evoked Ca^{2+} puffs

We next examined the effects of basal cytosolic $[Ca^{2+}]$ elevations on local Ca^{2+} puffs. For this purpose oocytes were loaded with EGTA (final intracellular concentration 300 μM) to suppress generation of Ca^{2+} waves by inhibiting inter-cluster diffusion of Ca^{2+} ions [23]. We further employed wide-field fluorescence microscopy to image a $40\mu m \times 40\ \mu m$ field of view with a fast (500 frames per s) electron-multiplied CCD camera, so as to sample many more puff sites than possible by one-dimensional linescan imaging. Figure 2 shows the experimental protocol (Figure 2A, a), and representative fluorescence traces monitored from small regions of interest centred on puff sites illustrating the responses evoked by photoreleased InsP_3 at resting cytosolic Ca^{2+} (Figure 2A, b) and when Ca^{2+} was elevated by Ca^{2+} influx (Figure 2A, c and d). The photolysis flash was delivered 4 s after the onset of the hyperpolarizing pulse so as to allow cytosolic $[Ca^{2+}]$ to equilibrate, and puffs were then recorded for 6 s while the hyperpolarization was maintained. We varied the duration of the photolysis flash to evoke differing numbers of puffs at resting cytosolic $[Ca^{2+}]$; 'weak' flashes (25–50 ms) were chosen to evoke on average about a single puff in the entire imaging field 40 $\mu m \times 40\ \mu m$, and 'strong' flashes (50–100 ms) to evoke up to four puffs. Even the 'strong' stimulus was chosen to evoke responses well below the maximal, so as to avoid possible saturation effects when responses were further potentiated by Ca^{2+} influx.

Figure 2(B) shows a scatter plot of the relationship between the numbers of individual sites in the imaging field where puffs were observed during 6 s following photorelease of InsP_3 as a function of the elevation of cytosolic $[Ca^{2+}]$ evoked by hyperpolarizing pulses. We express the $[Ca^{2+}]$ elevation in terms of fluorescence ratio change, without correction for oocyte autofluorescence (about 50 % of resting fluo-4 fluorescence). On the

(**A**) a, Schematic diagram of the experimental protocol. b and c, Representative fluorescence profiles of puffs evoked without (control) and with (+ influx) basal cytosolic $[Ca^{2+}]$ elevation, obtained from the same oocyte. The record in b was obtained from the single responding site within the image field, whereas the one in c shows superimposed traces from seven responding sites. d, Zoomed version of c on an expanded timescale to illustrate more clearly the variation in puff latencies following photorelease of InsP_3. The traces in b–d are blanked out during the photolysis flash. (**B**) Scatter plot showing the numbers of sites within the imaging field that showed puffs following weak (○; 25–50 ms flash duration) or strong (■; 50–100 ms) photorelease of InsP_3 as a function of cytosolic Ca^{2+} elevation during influx ($\Delta F/F_0[Ca^{2+}]_{cyt}$). (**C**) Mean numbers of responding puff sites within imaging field, grouped by photolysis strength and by elevation of basal cytosolic $[Ca^{2+}]$ ($\Delta F/F_o < 0.1$ or > 0.1).

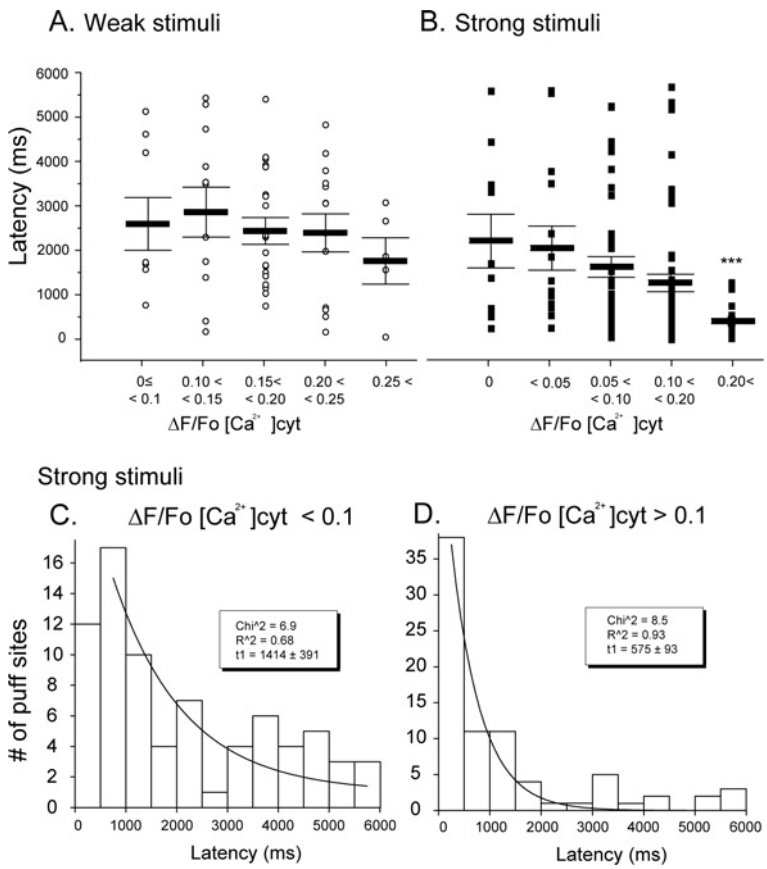

Figure 3 Puff latencies shorten with increasing cytosolic [Ca^{2+}]

Latencies were measured as the time from the end of the photolysis flash to the observation of the first puff at a given site. (**A** and **B**) Mean latencies of puffs evoked by weak and strong photorelease of InsP_3. (**C** and **D**) Histograms showing distributions of latencies of puffs evoked by strong stimuli during cytosolic Ca^{2+} elevations $<0.1\Delta F/F_o$ (**C**) and >0.1 (**D**). Curves are single exponential fits to the data with respective time constants of 1414 ± 391 ms and 575 ± 93 ms.

basis of the calibration described in the Experimental section, an increase in $\Delta F/F_o$ of 0.1 corresponds to a rise in [Ca^{2+}] of about 36 nM. With both weak and strong photolysis flashes the number of responding puff sites increased steeply with increasing basal cytosolic [Ca^{2+}], with strong flashes giving greater numbers at any given basal [Ca^{2+}]. Figure 2(C) shows mean data, grouped according to flash duration and whether basal cytosolic levels just before the photolysis flash were at or close to the resting level ($\Delta F/F_0 = 0$–0.1) or were appreciably elevated ($\Delta F/F_o > 0.1$).

Elevated cytosolic [Ca^{2+}] shortens puff latency

Figures 3(A) and 3(B) show scatter plots of individual and mean latencies of puffs, grouped according to the cytosolic [Ca^{2+}] elevation at the time of the photolysis flash. Puffs evoked by weak stimuli arose with relatively long (2–3 s) latencies, which tended to shorten with increasing cytosolic [Ca^{2+}], but did not show a statistically significant correlation (Figure 3A). On the other hand, mean puff latencies were shorter with stronger photorelease of InsP_3 (Figure 3B) and showed a marked dependence on cytosolic [Ca^{2+}], reducing from 2133 ± 200 ms at near resting level ($\Delta F/F_0 < 0.1$) to 1240 ± 174 ms when the fluorescence was elevated to >0.1 $\Delta F/F_0$ during Ca^{2+} influx ($P < 0.01$). Puff latencies followed roughly exponential distributions at both relatively low and high cytosolic [Ca^{2+}] (Figures 3C and 3D respectively), with a markedly shorter time constant at higher [Ca^{2+}].

Puff amplitudes are only weakly dependent on cytosolic [Ca^{2+}]

Next, we analysed the effects of changes in cytosolic [Ca^{2+}] on puff amplitudes. After pooling data across all different basal cytosolic [Ca^{2+}] levels we found no significant difference in mean puff amplitudes evoked by weak or strong photorelease of InsP_3 (Figure 4A; weak flash mean puff amplitude $\Delta F/F_o = 0.43 \pm 0.04$, $n = 56$ and strong flash $\Delta F/F_o = 0.42 \pm 0.03$, $n = 155$, $P > 0.05$). Looking then at the effect of elevating cytosolic [Ca^{2+}] levels, we observed little or no effect on the amplitudes of puffs evoked by weak photorelease (Figure 4B). On the other hand, puffs evoked by strong photorelease of InsP_3 showed a significant increase in puff amplitude with higher elevations of cytosolic [Ca^{2+}] ($\Delta F/F_o > 0.2$) (Figure 4C).

Puff durations are independent of basal cytosolic [Ca^{2+}]

We had observed previously a prolongation of puff duration when puffs were evoked after loading ER Ca^{2+} stores by inducing a prior Ca^{2+} influx in oocytes transfected to overexpress SERCA (sarcoplasmic/ER Ca^{2+}-ATPase), but not in control (non-expressing) oocytes. We now examined the effect of elevated $[Ca^{2+}]_{cyt}$ on puff duration. Puffs evoked by strong photorelease of InsP_3 were compared in the same imaging field at basal $[Ca^{2+}]_{cyt}$ and during induction of Ca^{2+} influx. Figure 5(A) shows a scatter plot of durations of puffs [measured as FDHM (full duration at half-maximal amplitude)] against the latency of the puffs

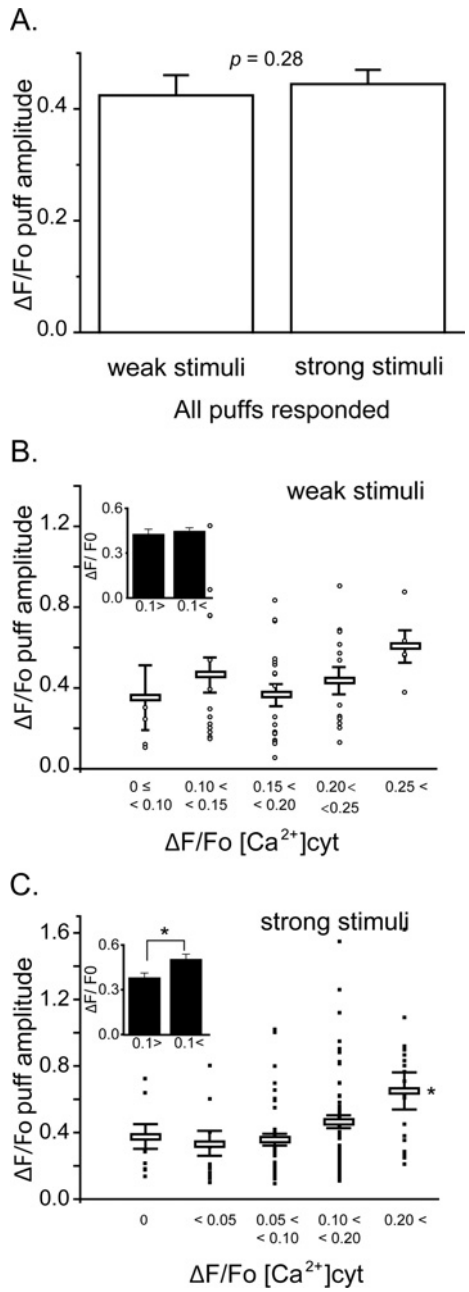

Figure 4 The amplitude of InsP_3-evoked puffs is only weakly dependent on the basal cytosolic [Ca^{2+}]

(**A**) Mean puff amplitudes evoked by weak photorelease of InsP_3 ($\Delta F/F_0 = 0.42 \pm 0.04$, $n = 56$) and strong photorelease ($\Delta F/F_0 = 0.44 \pm 0.23$, $n = 146$, $P > 0.05$), after pooling data across all basal cytosolic [Ca^{2+}] levels. (**B**) A scatter plot of amplitudes ($\Delta F/F_0$) of puffs evoked by weak photorelease of InsP_3 as a function of the increase in basal fluorescence during Ca^{2+} influx. ○, data from individual puffs. Error bars show means ± S.E.M. (**C**) Corresponding measurements of puff amplitudes following strong photorelease of InsP_3. The insets in (**B**) and (**C**) represent the mean values of puff amplitudes evoked by weak and strong photolysis flashes respectively grouped for cytosolic [Ca^{2+}] elevations <0.1 and >0.1 $\Delta F/F_0$.

following the UV flash. No differences were apparent in puff durations between the control and Ca^{2+} influx records, and puff durations did not show any obvious systematic dependence on latency following the UV flash. Figure 5(B) further plots mean values of FDHM of control puffs and puffs during Ca^{2+} influx, showing no significant difference ($P = 0.64$).

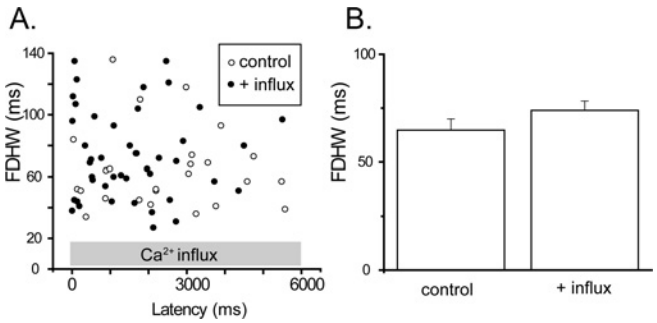

Figure 5 Duration of InsP_3-evoked puffs is independent on the basal cytosolic [Ca^{2+}]

(**A**) Scatter plot showing FDHM of all puffs observed within the imaging field as a function of their latencies. ○, control puffs evoked by the strong photolysis flash; ●, FDHM of puffs observed during Ca^{2+} influx (mean $\Delta F/F_0[Ca^{2+}]_{cyt} = 0.23 \pm 0.03$ for four trials). (**B**) Mean FDHM of puffs (control FDHM = 64.8 ± 5.2, $n = 25$, and with influx FDHM = 64.8 ± 5.2, $n = 44$; four oocytes).

DISCUSSION

The aim of the present study was to investigate how elevated basal cytosolic [Ca^{2+}] would affect InsP_3-evoked Ca^{2+} signals. We utilized the expression of Ca^{2+}-permeable nicotinic receptor/channels in the plasma membrane as a means to evoke controlled entry of extracellular Ca^{2+} into the cell during hyperpolarizing voltage-clamped pulses. Consistent with previous observations [4,5], we confirmed that cytosolic [Ca^{2+}] elevations powerfully facilitated InsP_3-mediated Ca^{2+} waves in terms of increased peak amplitude and shortened latency (Figures 1A and 1B). We further investigated the effect of elevated basal $[Ca^{2+}]_{cyt}$ on the local InsP_3-mediated Ca^{2+} puffs that are the triggers and fundamental building blocks of Ca^{2+} waves, as well as serving signalling functions in their own right. Our results show that the numbers of puff sites that respond at a given [InsP_3] are strongly potentiated in a graded manner with increasing $[Ca^{2+}]_{cyt}$, and that the mean latency of puffs markedly shortens. In contrast, puff amplitudes were little affected except at high $[Ca^{2+}]_{cyt}$ and we observed no significant effects of $[Ca^{2+}]_{cyt}$ on puff duration.

The effects we describe on InsP_3-evoked Ca^{2+} liberation from the ER can be directly attributed to changes in basal $[Ca^{2+}]_{cyt}$, and not to any increase in Ca^{2+} store filling within the ER. We had previously utilized Ca^{2+} influx through nicotinic receptors as a means to increase ER Ca^{2+} loading, by applying a transient hyperpolarizing pulse and then allowing $[Ca^{2+}]_{cyt}$ to subside to the resting level before examining responses to photoreleased InsP_3. However, changes in puff properties were observed only when SERCA activity was accelerated by cADP ribose [20,24] or when SERCA 2b was overexpressed [18]. With basal SERCA activity, no significant changes in puff triggering, kinetics or amplitude were apparent following even strong Ca^{2+} influx.

We have proposed that the puff is itself triggered by the stochastic opening of a single InsP_3R channel within the cluster [25,26]. Factors that determine the occurrence of puffs thus include the number of channels present in the cluster and the open probability of each channel. The latter, in turn, is a function of the concentrations of InsP_3 and Ca^{2+}, acting as co-agonists to open the channel [3,7,27]. Concordant with this mechanism, increasing [InsP_3] results in an increased frequency of puffs and a shortening of the latency to the first puff evoked at a site following photorelease of InsP_3 [26,28]). Similarly, modest

elevations of $[Ca^{2+}]_{cyt}$ will increase the open channel probability at a given $[Ins P_3]$, and hence increase the probability of puff triggering leading to a greater number of sites that generate puffs following photorelease of $Ins P_3$ and a shortening in mean latency of these puffs. Although gating of the $Ins P_3R$ channel is biphasically regulated by $[Ca^{2+}]$, inhibition of the native *Xenopus* $Ins P_3R$ arises only when $[Ca^{2+}]$ exceeds a concentration of several hundred micromolar [27] and thus would not be expected to be apparent in our experiments, where we estimate that the maximal Ca^{2+} influx ($\Delta F/F_o \sim 0.3$) corresponded to an increase in $[Ca^{2+}]_{cyt}$ of <100 nM.

Because the resting $[Ca^{2+}]_{cyt}$ is very low, small elevations above this level will strongly potentiate puff triggering. On the other hand, once an initial 'trigger' channel opens, the Ca^{2+} flux passing through it will elevate the local free $[Ca^{2+}]$ at the puff site to much higher levels, predicted to reach a concentration of a few hundred micromolar at the mouth of the open channel and at least several micromolar at the neighbouring $Ins P_3R$ within the cluster [29]. This will effectively 'swamp' the effect of any smaller elevation of basal $[Ca^{2+}]$. Once triggered, the puff thus becomes a self-regenerative process and its subsequent evolution is expected to be substantially independent of the preceding conditions; this is the probable explanation as to why we found little dependence of puff amplitudes and kinetics on basal $[Ca^{2+}]_{cyt}$.

The sensitization of global Ca^{2+} waves by elevated basal $[Ca^{2+}]_{cyt}$ may similarly be explained by enhanced coupling between neighbouring release sites. Ca^{2+} waves propagate because Ca^{2+} released from one site diffuses to evoke CICR from adjacent sites [11,12], and this triggering will be facilitated if $[Ca^{2+}]_{cyt}$ is already elevated. The results in Figure 1 were obtained using relatively weak photorelease of $Ins P_3$ that evoked only abortive Ca^{2+} waves, and basal $[Ca^{2+}]$ elevation promoted a more robust propagation by CICR resulting in strong potentiation of the spatially averaged Ca^{2+} signal. With stronger stimulation by $Ins P_3$ the amplitude of repetitive Ca^{2+} waves is not potentiated by Ca^{2+} influx [17], presumably because the more substantial Ca^{2+} release through $Ins P_3R$ swamps any effect of the elevated basal $[Ca^{2+}]$, but wave velocities and frequency of repetitive spikes are increased [17].

$Ins P_3$-mediated Ca^{2+} signalling can function as a coincidence detector, whereby release of Ca^{2+} from intracellular stores is potentiated by extracellular Ca^{2+} entering through plasmalemmal ligand- or voltage-operated channels. This interaction may arise through two different mechanisms, operating on different timescales. Most directly, as we describe in the present paper, elevation of basal $[Ca^{2+}]_{cyt}$ enhances the probability of triggering local and global $[Ca^{2+}]$ signals by binding to activating sites on the cytosolic face of the $Ins P_3R$. In addition, we have described a more circuitous mechanism, whereby extracellular $[Ca^{2+}]$ entering the cytosol is taken up by the action of SERCA pumps, leading to enhanced filling of ER Ca^{2+} stores [18]. That, in turn, promotes Ca^{2+} puffs and waves, probably because increased Ca^{2+} flux through the $Ins P_3R$ channel enhances CICR via the cytosolic activating sites on the $Ins P_3R$, and possibly also through luminal regulation of $Ins P_3R$ function [30–32]. The direct action of Ca^{2+} influx on $Ins P_3R$ is immediate and short lasting, depending on clearance rate from the cytosol. In contrast, potentiation via ER store filling is slower to develop, more persistent and subject to potential modulation by other messenger pathways, such as cADPR, that affect SERCA activity either directly or indirectly [20,33,34]. Interactions between these different modulatory mechanisms are likely to be of particular importance for Ca^{2+} signalling in neurons with regard to activity-dependent synaptic plasticity as well as gene expression and protein synthesis [35–37].

AUTHOR CONTRIBUTION

Michiko Yamasaki-Mann designed experiments, performed research, analysed the data and wrote the paper. Angelo Demuro performed research. Ian Parker designed experiments and wrote the paper.

FUNDING

This work was supported by the National Institutes of Health [grant number GM048071].

REFERENCES

1 Iino, M. (1990) Biphasic Ca^{2+} dependence of inositol 1,4,5-trisphosphate-induced Ca^{2+} release in smooth muscle cells of the guinea pig taenia caeci. J. Gen. Physiol. **95**, 1103–1122
2 Bezprozvanny, I., Watras, J. and Ehrlich, B. E. (1991) Bell-shaped calcium-response curves of Ins(1,4,5)*P*3- and calcium-gated channels from endoplasmic reticulum of cerebellum. Nature **351**, 751–754
3 Finch, E. A., Turner, T. J. and Goldin, S. M. (1991) Calcium as a coagonist of inositol 1,4,5-trisphosphate-induced calcium release. Science **252**, 443–446
4 Yao, Y. and Parker, I. (1992) Potentiation of inositol trisphosphate-induced Ca^{2+} mobilization in *Xenopus* oocytes by cytosolic Ca^{2+}. J. Physiol. **458**, 319–338
5 DeLisle, S. and Welsh, M. J. (1992) Inositol trisphosphate is required for the propagation of calcium waves in *Xenopus* oocytes. J. Biol. Chem. **267**, 7963–7966
6 Marshall, I. C. and Taylor, C. W. (1993) Biphasic effects of cytosolic Ca^{2+} on Ins(1,4,5)P_3-stimulated Ca^{2+} mobilization in hepatocytes. J. Biol. Chem. **268**, 13214–13220
7 Marchant, J. S. and Taylor, C. W. (1997) Cooperative activation of IP_3 receptors by sequential binding of IP_3 and Ca^{2+} safeguards against spontaneous activity. Curr. Biol. **7**, 510–518
8 Parker, I., Choi, J. and Yao, Y. (1996) Elementary events of Ins*P*3-induced Ca^{2+} liberation in *Xenopus* oocytes: hot spots, puffs and blips. Cell Calcium **20**, 105–121
9 Parker, I. and Yao, Y. (1996) Ca^{2+} transients associated with openings of inositol trisphosphate-gated channels in *Xenopus* oocytes. J. Physiol. **491**, 663–668
10 Parker, I. and Yao, Y. (1991) Regenerative release of calcium from functionally discrete subcellular stores by inositol trisphosphate. Proc. Biol. Sci. **246**, 269–274
11 Marchant, J. S. and Parker, I. (2001) Role of elementary Ca^{2+} puffs in generating repetitive Ca^{2+} oscillations. EMBO J. **20**, 65–76
12 Dawson, S. P., Keizer, J. and Pearson, J. E. (1999) Fire-diffuse-fire model of dynamics of intracellular calcium waves. Proc. Natl. Acad. Sci. U.S.A. **96**, 6060–6063
13 Parker, I. and Ivorra, I. (1990) Inhibition by Ca^{2+} of inositol trisphosphate-mediated Ca^{2+} liberation: a possible mechanism for oscillatory release of Ca^{2+}. Proc. Natl. Acad. Sci. U.S.A. **87**, 260–264
14 Mak, D. O., Pearson, J. E., Loong, K. P., Datta, S., Fernandez-Mongil, M. and Foskett, J. K. (2007) Rapid ligand-regulated gating kinetics of single inositol 1,4,5-trisphosphate receptor Ca^{2+} release channels. EMBO Rep. **8**, 1044–1051
15 Lechleiter, J. D. and Clapham, D. E. (1992) Molecular mechanisms of intracellular calcium excitability in *X. laevis* oocytes. Cell **69**, 283–294
16 Meyer, T. (1991) Cell signaling by second messenger waves. Cell **64**, 675–678
17 Yao, Y. and Parker, I. (1994) Ca^{2+} influx modulation of temporal and spatial patterns of inositol trisphosphate-mediated Ca^{2+} liberation in *Xenopus* oocytes. J. Physiol. **476**, 17–28
18 Yamasaki-Mann, M. and Parker, I. (2011) Enhanced ER Ca^{2+} store filling by overexpression of SERCA2b promotes IP_3-evoked puffs. Cell Calcium **50**, 36–41
19 Demuro, A. and Parker, I. (2005) 'Optical patch-clamping': single-channel recording by imaging Ca^{2+} flux through individual muscle acetylcholine receptor channels. J. Gen. Physiol. **126**, 179–192
20 Yamasaki-Mann, M., Demuro, A. and Parker, I. (2009) cADPR stimulates SERCA activity in *Xenopus* oocytes. Cell Calcium **45**, 293–299
21 Parker, I., Callamaras, N. and Wier, W. G. (1997) A high-resolution, confocal laser-scanning microscope and flash photolysis system for physiological studies. Cell Calcium **21**, 441–452
22 Martin, V. V., Beierlein, M., Morgan, J. L., Rothe, A. and Gee, K. R. (2004) Novel fluo-4 analogs for fluorescent calcium measurements. Cell Calcium **36**, 509–514
23 Dargan, S. L. and Parker, I. (2003) Buffer kinetics shape the spatiotemporal patterns of IP_3-evoked Ca^{2+} signals. J. Physiol. **553**, 775–788
24 Yamasaki-Mann, M., Demuro, A. and Parker, I. (2010) Modulation of endoplasmic reticulum Ca^{2+} store filling by cyclic ADP-ribose promotes inositol trisphosphate (IP_3)-evoked Ca^{2+} signals. J. Biol. Chem. **285**, 25053–25061
25 Rose, H. J., Dargan, S., Shuai, J. and Parker, I. (2006) 'Trigger' events precede calcium puffs in *Xenopus* oocytes. Biophys. J. **91**, 4024–4032

26 Dickinson, G. D., Swaminathan, D. and Parker, I. (2012) The probability of triggering calcium puffs is linearly related to the number of inositol trisphosphate receptors in a cluster. Biophys. J. **102**, 1826–1836
27 Foskett, J. K., White, C., Cheung, K. H. and Mak, D. O. (2007) Inositol trisphosphate receptor Ca^{2+} release channels. Physiol. Rev. **87**, 593–658
28 Shuai, J., Pearson, J. E., Foskett, J. K., Mak, D. O. and Parker, I. (2007) A kinetic model of single and clustered IP_3 receptors in the absence of Ca^{2+} feedback. Biophys. J. **93**, 1151–1162
29 Ullah, G., Parker, I., Mak, D. O. and Pearson, J. E. (2012) Multi-scale data-driven modeling and observation of calcium puffs. Cell Calcium **52**, 152–160
30 Horne, J. H. and Meyer, T. (1995) Luminal calcium regulates the inositol trisphosphate receptor of rat basophilic leukemia cells at a cytosolic site. Biochemistry **34**, 12738–12746
31 Sienaert, I., De Smedt, H., Parys, J. B., Missiaen, L., Vanlingen, S., Sipma, H. and Casteels, R. (1996) Characterization of a cytosolic and a luminal Ca^{2+} binding site in the type I inositol 1,4,5-trisphosphate receptor. J. Biol. Chem. **271**, 27005–27012

Received 9 August 2012/13 September 2012; accepted 4 October 2012
Published as BJ Immediate Publication 4 October 2012, doi:10.1042/BJ20121271

32 Higo, T., Hattori, M., Nakamura, T., Natsume, T., Michikawa, T. and Mikoshiba, K. (2005) Subtype-specific and ER lumenal environment-dependent regulation of inositol 1,4,5-trisphosphate receptor type 1 by ERp44. Cell **120**, 85–98
33 Lukyanenko, V., Gyorke, I., Wiesner, T. F. and Gyorke, S. (2001) Potentiation of Ca^{2+} release by cADP-ribose in the heart is mediated by enhanced SR Ca^{2+} uptake into the sarcoplasmic reticulum. Circ. Res. **89**, 614–622
34 Macgregor, A. T., Rakovic, S., Galione, A. and Terrar, D. A. (2007) Dual effects of cyclic ADP-ribose on sarcoplasmic reticulum Ca^{2+} release and storage in cardiac myocytes isolated from guinea-pig and rat ventricle. Cell Calcium **41**, 537–546
35 Rose, C. R. and Konnerth, A. (2001) Stores not just for storage. intracellular calcium release and synaptic plasticity. Neuron **31**, 519–522
36 Barbara, J. G. (2002) IP_3-dependent calcium-induced calcium release mediates bidirectional calcium waves in neurons: functional implications for synaptic plasticity. Biochim. Biophys. Acta **1600**, 12–18
37 Watanabe, S., Hong, M., Lasser-Ross, N. and Ross, W. N. (2006) Modulation of calcium wave propagation in the dendrites and to the soma of rat hippocampal pyramidal neurons. J. Physiol. **575**, 455–468